# Power Exhaust in Next-Step Fusion Devices

T. Hartmann[1], H. Zohm[1]

[1] *Max-Planck Institut für Plasmaphysik, Garching, Germany*

**Abstract**

With a 0-D systems code the power exhaust in a next-step fusion device that is based on the PPCS-B design was analysed. Especially the enhancement of the core radiation by means of core impurity seeding in two different scenarios (constant temperature and constant total normalised plasma beta) was investigated. The results indicate that this method improves the situation in the divertor, but comes along with an unfavourable economical burden.

## 1. Introduction

The power exhaust is a key driver in the design of a next-step fusion device. Especially the conducted power flux in the SOL to the divertor region constrains the design options. One idea to overcome this problem is to increase the impurity content in the plasma core, so that the power conducted through the separatrix and finally to the divertor plates is reduced by enhanced radiation in the plasma core.

## 2. Model and Methods

To analyse the reduction of the heat load on the divertor plates via radiation in the plasma core and mantle we used a 0-D systems code with modules for each component of a fusion reactor. The main elements of the physics module are balances for power, particles, pressure and current. Thus it is possible to solve the underlying equations in a self-consistent way (see also [1], [2], [3] and [4]). A detailed description of the systems code is in progress [5]. For the analysis a fusion device that is based on the PPCS-B design was used [6]. The basic parameters of this reactor are listed in table 1. We fixed the main machine parameters (major radius, magnetic field, etc.) and increased the impurity content stepwise to enhance radiation in the plasma core and mantle. The latter is defined as the region between the core and the separatrix (i.e. normalised minor radius $\rho = r/a$: $\rho_{core} < \rho < 1$). Furthermore, two different scenarios for the analysis were chosen where either the mean temperature (Case I: $\langle T \rangle = 20\text{keV}$) or the total normalised plasma beta (Case II: $\beta_N = 3.5$) is kept constant. Here we assumed that ideal MHD limits the achievable total $\beta_N = \beta_{N,th} + \beta_{N,fast}$, a pessimistic assumption that is still under discussion.

| | |
|---|---|
| $R_0$ | 8.6 m |
| $A$ | 3.0 |
| $\kappa_{95}$ | 1.7 |
| $\delta_{95}$ | 0.25 |
| $V$ | 2380 $m^3$ |
| $q_{95}$ | 3.0 |
| $I_p$ | 28 MA |

| | |
|---|---|
| $B_t$ | 6.9 T |
| $\tau_E$ | IPB98(y,2) |
| H | 1.2 |
| $\tau_p^*/\tau_E$ | 5 |
| $n_{GW}$ | $1.08 \cdot 10^{20} m^{-3}$ |
| $n_0/n_{ped}$ | 1.5 |
| $n_{sep}$ | $0.3 \cdot 10^{20} m^{-3}$ |

| | |
|---|---|
| $r_{syn}$ | 0.7 |
| $\rho_{core}$ | 0.95 |
| $\tau_{pulse}$ | $\infty$ |
| $q_{div}^{max}$ | 10 $MW/m^2$ |
| $f_{neutron}^{mult}$ | 1.39 |
| $\eta_{thermal}$ | 40.5% |
| $\eta_{H\&CD}$ | 60% |

**Table 1.** Parameters of the PPCS-B-like device used in the study.

For density and temperature, parabolic profiles with a linear decrease from pedestal to separatrix values were used (see also [3]). Moreover, it was assumed that the Greenwald density limit is an edge phenomenon. Thus the electron density at the pedestal was fixed at the Greenwald density [7] and we allowed for finite density peaking at the low collisionality expected for a next-step fusion device [8]. The temperature at the pedestal was adjusted subsequently so that the pedestal pressure matches with a scaling expression [9]. The separatrix temperature was calculated with a simple 2-point model [10] and the temperature peaking $T_0/T_{ped}$ was adapted according to the particular scenario. In both cases Argon as seeded impurity was selected and its fraction $f_{Ar} = n_{Ar}/n_e$ compared to the electron density was increased stepwise from 0.7% to 2.1%.

## 3. Results and Discussion

Figure 1 shows the divertor radiation fraction, defined as that part of the power flux at the separatrix which is radiated in the divertor region. It was adjusted to keep the peak power flux to the outer divertor plates below 10 $MW/m^2$. As could be expected, in case I the divertor radiation fraction decreases as the Argon fraction is increased. This means that a higher core radiation shifts the divertor radiation to a more feasible regime. The core radiation is a combination of synchrotron, Bremsstrahlung and line radiation (Fig. 2).

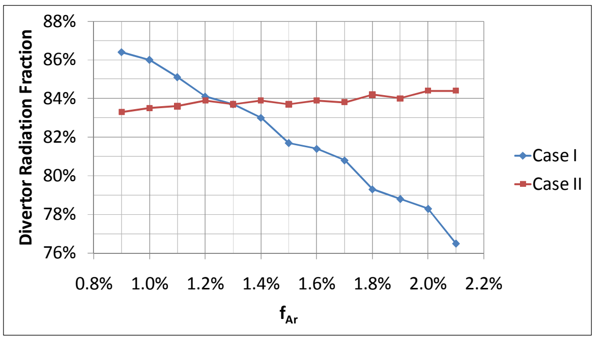


**Figure 1.** Radiation fraction in the divertor region for case I ($\langle T \rangle$ = const.) and case II ($\beta_N$ = const.).

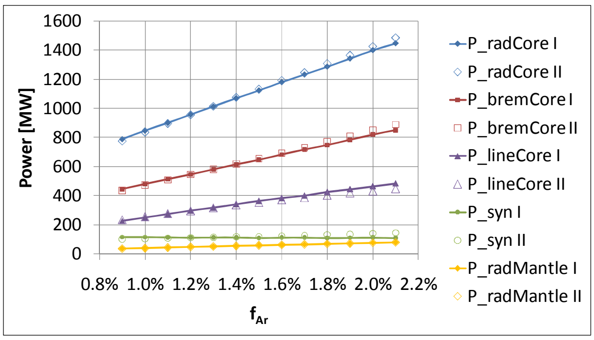


**Figure 2.** Radiation losses in core and mantle region for case I ($\langle T \rangle$ = const.) and case II ($\beta_N$ = const.).

In contradiction, in case II the divertor radiation fraction keeps nearly constant, it even slightly increases (Fig. 1). The reason is that in this case the plasma pressure and accordingly the temperature must rise to keep $\beta_N$ constant, because of the constant electron density. The normalised total plasma beta consists of a thermal and a fast particle part. The latter one is approximately proportional to $n_{DT}^2 \cdot T$ and decreases by an increasing fuel dilution and consequently increasing Argon fraction [11]. This means that the thermal part must increase disproportionately, which in turn causes an increase of $W_{th}$ and concomitant of $P_{con}$ (Fig. 4). However, the enhanced radiation in the mantle region is just able to compensate this increase so that finally $P_{sep} = P_{con} - P_{radMantle}$ remains nearly constant (Fig. 4).

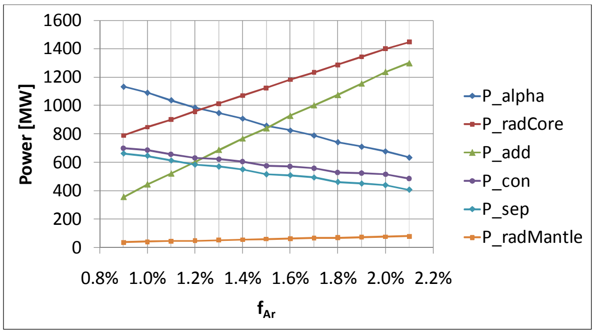


**Figure 3.** Power balance for case I ($\langle T \rangle$ = const.).

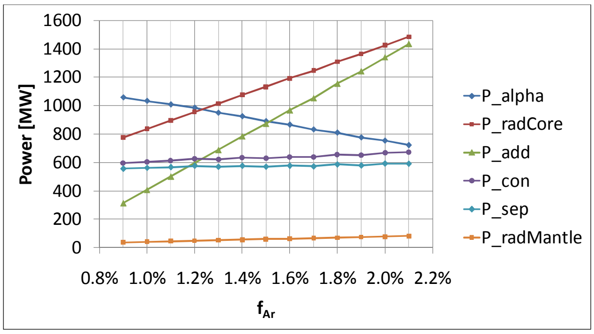


**Figure 4.** Power balance for case II ($\beta_N$ = const.).

As can be seen in figures 3 and 4, in both cases the increase of the core radiation caused by higher impurity content leads to an increase of the additional power $P_{add}$ needed to equalise the power balance in the core: $dW_{th}/dt = 0 = P_\alpha + P_{add} - P_{radCore} - P_{con}$

The additional power consists of the power to drive current in the plasma $P_{CD}$ and an external pure heating power $P_{heat}$ that is ideally zero. Whereas $P_{CD}$ remains nearly constant despite a slight decrease in case II, $P_{heat}$ increases to significant high values (Fig. 5). Therefore the recirculating electric power in the plant increases. This leads to a decrease of the net electric power output and makes the general balance more and more unfavourable (Fig. 6).

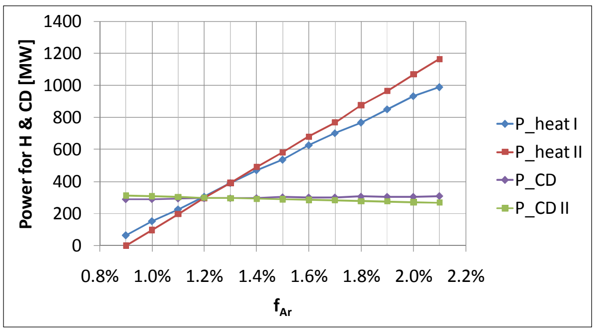


**Figure 5.** Heating and current drive power for case I ($\langle T \rangle$ = const.) and case II ($\beta_N$ = const.).

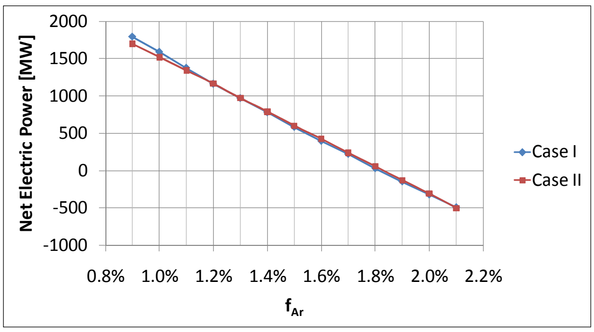


**Figure 6.** Net electric power output for case I ($\langle T \rangle$ = const.) and case II ($\beta_N$ = const.).

Thus it is advantageous for the general balance of the power plant that in both cases the fraction of Argon as seeded impurity is kept as small as possible. Otherwise the economical balance which is related to the net electricity power output to the grid gets more and more unattractive. Nonetheless, especially in case I, an enhancement of the core radiation by means of impurity seeding in the core improves the situation in the divertor. Finally, one should also pay attention to a possible degradation of the confinement caused by higher radiation in the plasma core, in particular to the H-mode threshold. In this study the operation points were all above at least two times this value.

## 4. Conclusions and Perspectives

This case study shows that it is unfavourable to increase the core radiation arbitrarily to secure the divertor plates. In case II this option seems to be even useless. A reasonable way is to use the limits set by materials or technology as constraints and to solve the equations in a self-consistent way with models for each component on similar levels of sophistication in the systems code. To enhance self-consistency in the systems code, it is planned to integrate a simple model for the divertor radiation fraction where non-coronal effects on the radiation losses are considered.

## Acknowledgments

The authors want to thank R. Dux, T. Eich, A. Kallenbach, O. Kardaun, K. Lackner, M. Wischmeier of the IPP Garching, R. Kemp, D. Ward of the CCFE Culham and T. Hamacher of the TU Munich for many fruitful discussions in the scope of this work.

## References

[1] H. Zohm, Fusion Science and Technology **58**, 613 (2010)
[2] D. Ward, SERF3/UKAEA/DFCA1.1 (2002)
[3] J. Johner, Fusion Science and Technology **59** (2), 308 (2011)
[4] Z. Dragojlovic et al, Fusion Engineering and Design **85** (2), 243 (2010)
[5] T. Hartmann, PhD-Thesis, to be published
[6] D. Maisonnier et al, Final Report of the European Fusion Power Plant Conceptual Study, EFDA (2005)
[7] M. Greenwald et al, Nuclear Fusion **28**, 2199 (1988)
[8] G. V. Pereverzev et al, Contributed Papers to 33th EPS Conf. on Plasma Physics, P-1.113 (2006)
[9] E. J. Doyle et al, Nuclear Fusion **47** (6), S18 (2007)
[10] P. C. Stangeby, The Plasma Boundary of Magnetic Fusion Devices. Bristol: Institute of Physics (2000)
[11] N. Uckan et al, ITER Physics Design Guidelines: 1989. ITER Doc. Series No. 10. (1990)